Off-Boresight Radiation from Impulse Radiating Antennas

J. Scott Tyo
EECE Department
University of New Mexico
Albuquerque, NM 87131-0001
tyo@ece.unm.edu

Everett G. Farr and L. H. Bowen
Farr Research, Inc.
614 Paseo del Mar NE
Albuquerque, NM 87123
{efarr,lhbowen}@farr-research.com

Jon S. H. Schoenberg
AFRL/DEHP
3550 Aberdeen SE
Kirtland AFB, NM 87117
schoenberg@ieee.org

***Abstract*— An analytic method for predicting off boresight radiated £elds from Impulse Radiating Antennas (IRAs) is developed in the time domain. This theory is used to examine the radiation pattern from common re¤ector IRA con£gurations both temporally and in the frequency domain. Various methods for controlling the sidelobes in the frequency domain are discussed. The results are compared with experimental measurements of a half IRA in the E- and H-planes.**

I. Introduction

Impulse radiating antennas (IRAs) are a class of focused aperture antennas that have been used extensively for the generation and radiation of ultra-wideband electromagnetic pulses [1]. Re¤ector IRAs are comprised of a non-dispersive, conically-symmetric TEM structure (transmission line) feeding a paraboloidal re¤ector. The re¤ector converts the outgoing spherical wave on the TEM feed into a plane wave in the near-£eld by the geometric optics approximation. A stereographic projection is used to map the mode structure of the conical TEM mode into a longitudinal TEM mode at the aperture plane for purposes of analysis. A schematic of a typical re¤ector IRA is shown in £g. 1.

The prompt radiated £elds on boresight from an IRA can be predicted by using the distribution of the TEM mode in the focused aperture of the antenna and considering aperture theory in the time or frequency domain. For the early time, the radiated £eld on boresight at position r and time t is given in the physical optics approximation as[1]

$$E_{rad} = \frac{h_a}{2\pi r c f_g}\frac{dV}{dt}, \tag{1}$$

where V is the applied voltage waveform and h_a is the aperture height given as

$$h_a = \frac{f_g}{V_0}\int\int_A E_y(x,y)dxdy. \tag{2}$$

In (2), $f_g = Z_{line}/\eta_0$, $\eta_0 = 120\pi\Omega$, is the geometric impedance factor, V_0 is the peak applied voltage, and A is the aperture.

The radiated £elds on boresight from an IRA are well understood. Relatively few investigations have focused on the radiation from these antennas in directions other than the direction of focus. IRAs were designed to radiate transient electromagnetic pulses, but the non-dispersive nature of IRAs

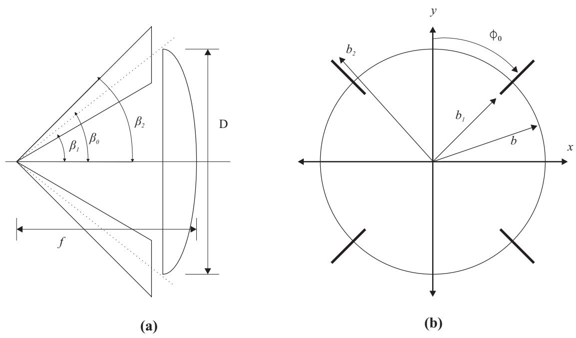

Fig. 1. Schematic of the IRA being studied. a) Side-view with focal length and diameter. b) Aperture plane after stereograhic projection. The electrodes are self reciprocal with respect to the circle $\rho = b$.

and their inherently wide (multiple decades) impedance bandwidth make IRAs attractive for multiband applications such as swept CW radar and frequency hopping radios. If IRAs are to be used for such broadband CW applications, then an understanding of the sidelobe performance is important.

In this paper, we investigate the off-boresight radiated £elds in the time and frequency domains for a handful of aperture con£gurations that have been shown to work well for the radiation of large prompt boresight £elds. The aperture con£gurations tested here have feed arms at either 45° or 60° from the horizontal. For each feed arm angle, there are three aperture con£gurations tested. The £rst is the most common con£guration, whereby the focused aperture coincides with the circle of symmetry of the feed arms. We term this the "standard (S)" con£guration. The second con£guration focuses the entire circle *inside* the feed arms. Such a con£guration is sub-optimal, but is necessary in some applications to enhance the mechanical strength of the IRA when the feed arms are not self supporting [2], [3]. We term this the "rigid (R)" con£guration. The third con£guration has the same maximum aperture curve, but the portions of the aperture with E-£elds that contribute destructively to the integral in (2) are eliminated. We term this the "trimmed (T)" con£guration. All feed con£gurations examined in this paper are for $Z_{line} = 200\Omega$, but the results are qualitatively similar for other impedances.

II. Physical Optics Model in the Time Domain

In order to predict the early-time, off-boresight radiation from an IRA, we turn to the theory of focused aperture antennas. The following analysis could proceed in either the time domain or the frequency domain. We present a direct time domain theory here that is valid on- and off-boresight.

Using conventional aperture theory, we assume short circuited aperture centered at the origin in the x-y plane and use image theory. Equivalent surface magnetic currents on the aperture can be impressed as

$$\mathbf{M}_s(x',y',t) = -2\hat{\mathbf{z}} \times \mathbf{E}_{TEM}(x',y',t), \tag{3}$$

where $\mathbf{E}_{TEM}$ is the electric £eld of the TEM mode. The primed coordinates indicate the aperture (source) point. Using the time domain Green's function for radiation in a uniform half space, the electric vector potential $\mathbf{F}$ at position $\mathbf{r}$ and time t is

$$\mathbf{F}(\mathbf{r},t) = \frac{\varepsilon}{4\pi} \iint_A \frac{\mathbf{M}_s(\mathbf{r}',t-R/c)}{R} dx'dy', \tag{4}$$

where $R = |\mathbf{r}-\mathbf{r}'|$ and c is the speed of light. The portion of $\mathbf{M}$ in the y-direction produces the cross-polarized radiated £eld, and the portion of the integrand in (6) in the x-direction produces the co-polarized £eld. Experimental results indicate that the cross polarized radiation is dominated manufacturing irregularities, not the aperture £elds. Cross-pol is ignored here.

We can approximate

$$R \approx r - \sin\theta\cos\phi x' - \sin\theta\sin\phi y', \tag{5}$$

and the part of (4) that produces the co-polarized £eld becomes

$$F_x = \frac{\varepsilon \iint_A E_y\left(x',y',t-r/c+\frac{\sin\theta\cos\phi x'+\sin\theta\sin\phi y'}{c}\right) dx'dy'}{2\pi r}. \tag{6}$$

The co-polarized radiated $\mathbf{E}_{co}$ £eld is obtained by taking the curl of $\mathbf{F}$ as

$$\begin{aligned}\mathbf{E}_{co} \;=\; & \tfrac{1}{2\pi rc}\left(\hat{\phi}\cos\theta\cos\phi+\hat{\theta}\sin\phi\right)\times \\ & \tfrac{d}{dt}\iint E_y\left(x',y',t-\tfrac{r}{c}+\tfrac{\sin\theta\cos\phi x'+\sin\theta\sin\phi y'}{c}\right)dx'dy'.\end{aligned} \tag{7}$$

We now use (7) to £nd the temporal radiated £eld in the E- and H-planes. In the H-plane we have $\phi = \{0,\pi\}$, and we compute the radiation as a function of the polar angle θ. If we assume an ideal step excitation, we obtain

$$E^h_\phi(r,\theta,t) \;=\; \frac{\cot\theta}{2\pi r}\int E_y\left(-\frac{ct'}{\sin\theta},y'\right)dy'. \tag{8}$$

In the above equation $t' = t - r/c$ is the retarded time at the center of the aperture. We de£ne the quantity $\Phi^h(x)$ as

$$\Phi^h(x) = (1/V_0)\int E_y(x,y')dy'. \tag{9}$$

Using (9), (8) becomes

$$E^h_\phi(r,\theta,t) = \frac{V_0\cot\theta}{2\pi r}\Phi^h\left(-\frac{ct'}{\sin\theta}\right). \tag{10}$$

A simlar analysis in the E-plane yields

$$E^e_\theta(r,\theta,t) = \frac{V_0}{2\pi r\sin\theta}\Phi^e\left(-\frac{ct'}{\sin\theta}\right), \tag{11}$$

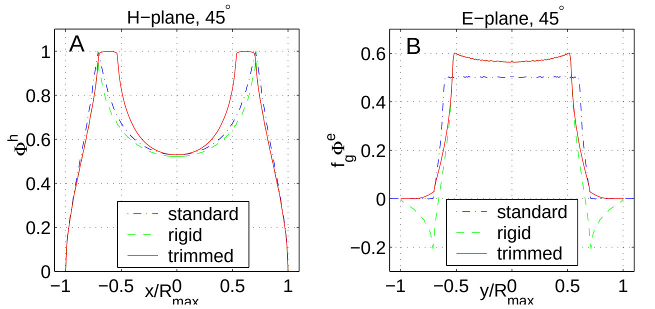

Fig. 2. A. $\Phi^h(x)$ and B. $\Phi^e(y)$ for the 45° feed arms, $Z = 200/,\Omega$. The position variables are normalized to the maximum radius. Φ^h is normalized to the electric scalar potential difference between the electrodes. Φ^e is normalized to the total magnetic scalar potential obtained in integrating around the electrodes.

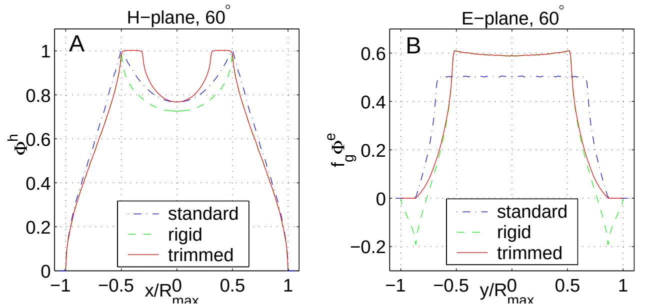

Fig. 3. A. $\Phi^h(x)$ and B. $\Phi^e(y)$ for the 60° feed arms, $Z = 200/,\Omega$. The normalization is as in £g. 2.

where

$$\Phi^e(y) = (1/V_0)\int E_y(x',y)dx'. \tag{12}$$

The computed values of $\Phi^h(x)$ and $\Phi^e(y)$ are shown in £g. 2 and £g. 3 for the 200 Ω IRA with 45° and 60° feed arms. When the voltage waveform applied to the IRA feed is not an ideal step, we must convolve the above results with the derivative of the applied voltage. It can be shown that (10) and (11) reduce to (1) on boresight.

III. Frequency Domain Sidelobe patterns

To £nd the sidelobes as a function of θ for a given frequency ω, we take the Fourier transforms of (10) and (11) to get

$$E^h_\phi(r,\theta,\omega) \;=\; \frac{V_0\cos\theta}{2\pi rc}\tilde{\Phi}^h\left(-\frac{\omega\sin\theta}{c}\right) \text{ and} \tag{13}$$

$$E^e_\theta(r,\theta,\omega) \;=\; \frac{V_0}{2\pi rc}\tilde{\Phi}^e\left(-\frac{\omega\sin\theta}{c}\right). \tag{14}$$

In the above equations, $\tilde{\Phi}(k)$ is the Fourier transform of $\Phi(x)$. We can £nally compute the effective gain in the E- and H-planes by dividing the local radiated power density using (13) and (14) by the average power density that would exist were all the power *available* to the antenna to be radiated isotropically. The total power on the antenna (assuming step excitation) is

$$P_{tot}(\omega) = \frac{1}{2\omega^2 Z_{line}}, \tag{15}$$

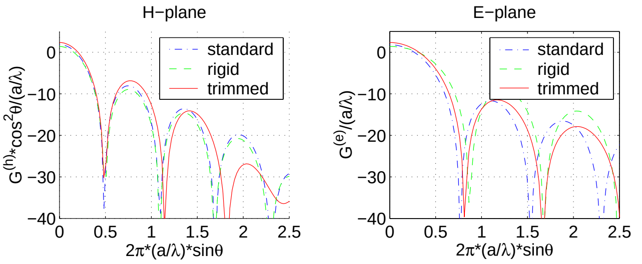

Fig. 4. Sidelobe patterns for the 45° feed arms in the E and H planes. The gain is normalized to the radius of the aperture (in wavelengths) squared. For example, to get the gain for an aperture that has a maximum radius of one wavelength, add 8.2 dB.

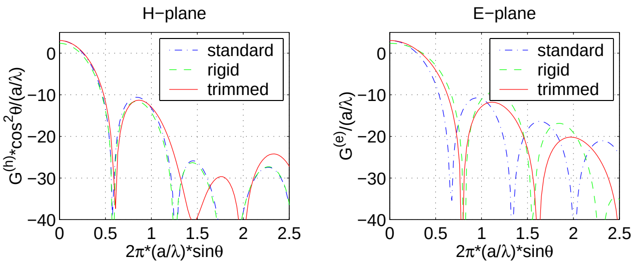

Fig. 5. Sidelobe patterns for the 60° feed arms in the E and H planes. The normalization is described in the caption to £g. 4.

and the effective gains in the E- and H- planes are

$$G^{(h)}(\theta,\omega) = 4\pi\cos^2\theta f_g \frac{f^2\left|\tilde{\Phi}^{(h)}\left(-\frac{\omega\sin\theta}{c}\right)\right|^2}{c^2} \tag{16}$$

$$G^{(e)}(\theta,\omega) = 4\pi f_g \frac{f^2\left|\tilde{\Phi}^{(e)}\left(-\frac{\omega\sin\theta}{c}\right)\right|^2}{c^2} \tag{17}$$

Examination of the Fourier transforms of Φ^e and Φ^h for the various con£gurations of interest determines the sidelobe performance in each case. These distributions are presented in £g. 4 and £g. 5 for the 45° and 60° feed arms, respectively. Eqn. (17) tells us that the antenna pattern *shape* is independent of frequency in the E-plane, and (16) says that the shape in the H-plane is invariant, except for an overall envelope weighting of $\cos^2\theta$. This is because the aperture illumination is identical for all frequencies (since the feed is TEM). The only change as a function of frequency is the *location* in angular space of the sidelobes. The key features of the sidelobe patterns are presented in table I.

We see from the table that the 60° con£gurations all provide approximately 1 dB of additional peak gain, depending on the con£guration of the aperture. A 1 dB increase in gain corresponds to a 10% increase in the radiated electric £eld. These results agree with previous numerical [4] and experimental [5] studies. We also see that the average sidelobe levels (SLL) are signi£cantly reduced for the 60° feed arms, especially in the H-plane, where we see a 4 - 5 dB reduction in SLL. This reduction in sidelobes comes at the expense of a slightly larger beamwidth.

TABLE I

SIDELOBE PERFORMANCE, GAIN AND 3 DB BEAMWIDTH. EFFECTIVE GAIN IS NORMALIZED TO THE SIZE OF THE APERTURE IN WAVELENGTHS.

ϕ_0	ap.	$\frac{G}{(a/\lambda)^2}$	H-plane		E-Plane	
			SLL	BW	SLL	BW
°		dB	dB	°	dB	°
45	S	3.55	9.90	4.71	13.5	6.82
45	R	3.12	10.3	4.41	10.56	8.86
45	T	4.08	9.2	4.41	13.83	7.37
60	S	4.78	13.7	5.00	13.8	5.78
60	R	4.10	14.0	5.40	11.7	7.87
60	T	4.78	14.3	5.40	14.9	6.89

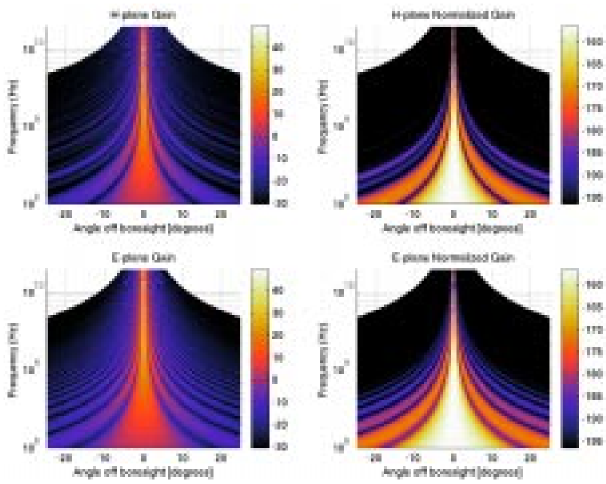

Fig. 6. Normalized gain (left column) and absolute gain (right column) for the trimmed aperture con£guration with $\phi_0 = 60°$.

Knowledge of Φ^h and Φ^e allows us to predict the antenna radiation pattern as a function of both angle and frequency. Example radiation patterns are presented for the 200 Ω trimmed con£gurations with $\phi_0 = 60°$ in £g. 6.

IV. EXPERIMENTAL MEASUREMENTS

A set of experimental measurements was collected using a half-IRA. A half-IRA is an IRA where the bottom half of the re¤ector and feed is replaced by a partial ground plane [6]. The early-time response of the half-IRA is predicted by (1) and (2), just as for the full IRA. The prompt off-boresight £elds are predicted by (10) and (11), with the appropriate forms of $\Phi^h(x)$ and $\Phi^e(y)$.

The half-IRA used in this study was a 100-Ω con£guration (half of a 200 Ω IRA) with $\phi_0 = 45°$. The diameter of the half-IRA was 1 m. The aperture was untrimmed, resulting in the "standard" aperture con£guration. The data were obtained directly in the time domain using a replicating TEM sensor with 2-ns clear time. The antenna was fed with a picosecond pulse labs 4015C pulser, which produced a -4 V amplitude step-like waveform with a 15 ps risetime. Data were measured with a Tektronix CSA 803A communcications signal anaylzer equipped with an SD-24 20-GHz sampling head.

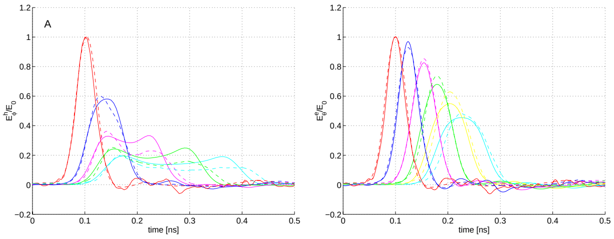

Fig. 7. Measured (dashed) and predicted (solid) E-£eld in the H-plane (A) and the E-plane (B). The peak £eld decreases monotonically off-boresight in both cases. Measurements and predictions were made at 0°, 1.25°, 2.5°, 3.75°, and 5° in the H-plane and 0°, 1.2°, 2.2°, 3.2°, 4.2°, and 5.2° in the E-plane.

The two antennas were mounted on camera tripods and positioned 26.6 m apart. The measurements were made over an arroyo (a dry creek bed) that delayed the ground-bounce signal, i. e. the re¤ected signal from the ¤at ground that appears delayed in time. The half IRA was then rotated in the E- and H-planes to obtain off-boresight measurements. The sensor was £xed throughout and oriented towards the feed point of the half-IRA. The measured responses are presented in £g. 7 in the H- and E-planes, and compared with the predictions made using (10) and (11).

The data presented in £g. 7 are normalized E-£eld values because the absolute sensitivity of the sensor was uncalibrated. Only relative comparisons could be made among the different off-boresight angles. The measured data were normalized to the peak boresight measured £eld, and the predicted data were normalized to the peak boresight predicted £elds. It is known that (1) and (2) tend to overpredict the peak £elds on boresight for re¤ector IRAs, possibly due to feed blockage that is ignored in the geometric optics approximations used to derive (1) and (2) [1].

V. Discussion and Conclusions

We see from the unnormalized gain plots that the peak boresight gain increases as f^2, as is the case for all ideal aperture antennas at high frequencies. This is predicted by (1), which has a time derivative of the applied voltage waveform equivalent to multiplying by $j\omega$ in the frequency domain). It is important to note that IRAs, like other aperture antennas *are not constant gain*. However, when excited by an ideal step function (which has energy content which varies like $1/f^2$) the radiated £eld is (approximately) impulsive. While the absolute gain does increase as f^2, the shapes of the sidelobe patterns are *independent* of frequency. This uniformity is due to the ultra-wideband nature of the feed structure. The aperture £elds are identical for all frequencies, so long as the higher order modes are insigni£cant.

The measured and predicted data presented in £g. 7 have good qualitative agreement, though there are noticeable differences. The relative values of the peak £elds and FWHM pulsewidths are reasonably well predicted by (10) and (11), though there are some shape differences between the predicted and measured waveforms. In the H-plane the agreement is excellent for both pulse width and peak radiated £eld ($<8\%$ error for all cases). In the E-plane, the trend is accurately predicted, but the agreement is not quite as good as in the H-plane.

The general two-peaked shape of the waveform in the H-plane is predicted by (10), though the asymmetrical shape of the measured response is not predicted. The reduced amplitude of the second peak might be due to asymmetric feed blockage. On boresight, the feed arms are very thin and are ignored in deriving the prompt response in (1) and (2). Off-boresight, the effect of the feed arms must be reintroduced, causing perturbations in the theory presented here. The subject of prompt and late-time feed blockage in IRAs is a topic for future investigation.

In this paper, we presented a physical optics theory for the time-domain, off-boresight radiated £elds of IRAs. We used the theory to predict and compare the sidelobe performance of common re¤ector IRAs with feed arms at 45° and 60° from the horizontal. The theory indicates that the sidelobe performance of the 60° IRA is signi£cantly better than the 45° IRAs. When coupled with earlier results that demonstrate a signi£cant improvement in boresight gain [4], [5] and cross polarization performance [5] for the 60° IRAs, it is clear that re¤ector IRAs with 60° feed arms are an improvement over the more traditional 45° IRAs.

The theoretical predictions were compared with measured data in the far-zone of a 1-m-dimater Half IRA with feed arms at 45°. Both theory and experiment indicate that the prompt radiated £eld in the H-plane has two peaks, while the radiated £eld in the E-plane has only one. The experimental measurements indicate asymmetries in the temporal response in the H-plane which aren't apparent in the theoretical data. We hypothesize that this might be due to asymmetric feed blockage off boresight, as the theory presented here completely neglects feed blockage.

References

[1] C. E. Baum, E. G. Farr, and D. V. Giri, "Review of impulse-radiating antennas," in *Review of Radio Science* (W. R. Stone, ed.), pp. 403–439, New York: Oxford U. Press, 1999.

[2] L. H. Bowen, E. G. Farr, J. P. Paxton, A. J. Witzig, C. E. Baum, D. I. Lawry, and W. D. Prather, "Fabrication and testing of a membrane IRA," in *Sensor and Simulation Notes #464* (C. E. Baum, ed.), Albuquerque, NM: Air Force Research Laboratory, 2002.

[3] L. M. Atchley, E. G. Farr, J. S. Tyo, N. de la Merced, and L. L. Altgilbers, "Development and testing of a parachute deployable impulse radiating antenna," in *Sensor and Simulation Notes #465* (C. E. Baum, ed.), Albuquerque, NM: Air Force Research Laboratory, 2002.

[4] J. S. Tyo, "Optimization of the TEM feed structure for four-arm re¤ector impulse radiating antennas," *IEEE Trans. Antennas Propagat.*, vol. 49, pp. 607–614, 2001.

[5] L. H. Bowen, E. G. Farr, C. E. Baum, T. C. Tran, and W. D. Prather, "Experimental results of optimizing the location of feed arms in a collapsible IRA and a solid IRA," in *Sensor and Simulation Notes #450* (C. E. Baum, ed.), Albuquerque, NM: Air Force Research Laboratory, 2000.

[6] C. E. Baum, "Variations on the impulse radiating antenna theme," in *Sensor and Simulation Notes #378* (C. E. Baum, ed.), Albuquerque, NM: Phillips Laboratory, 1995.